DETONATIONS AND SHOCK WAVES

Module Fundamentals of Hydrogen Safety

Lecture 10

THE HUGONIOT CURVE

THE HUGONIOT RELATIONS

- Relationships exist between the variables on the two sides of a shock wave. These are known as the Hugoniot relations.
- The Hugoniot relations establish the connection between eight quantities: four variables on the left (low pressure) side of the shock wave (p_0, h_0, ρ_0, v_0) and four variables on the right (high pressure) side ($p_\infty, h_\infty, \rho_\infty, v_\infty$).
- These variables are the solution to the inviscid conservation equations for mass, momentum, and energy for waves in a steady, constant area flow.
- There are three Hugoniot relations connecting eight quantities (four on either side of the shock wave).

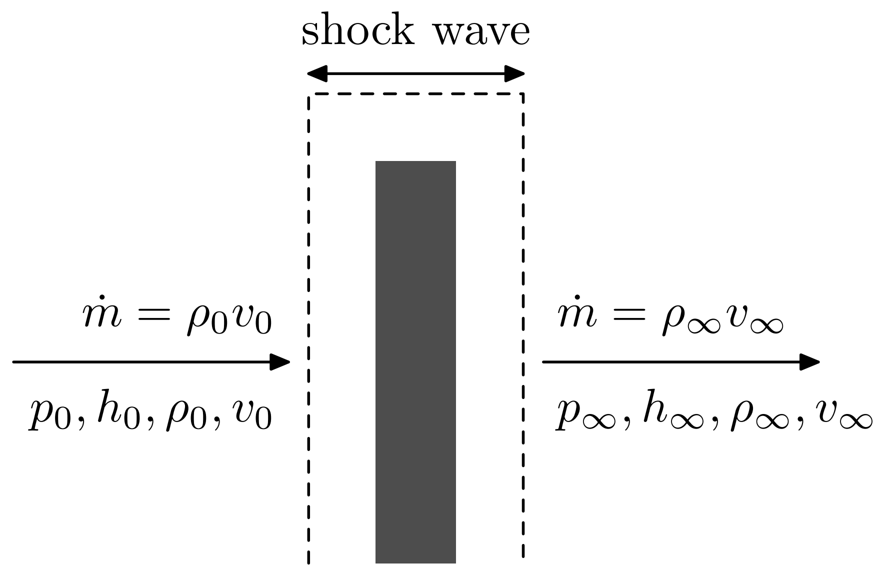

Figure 1: Simplified shock wave structure.

The Hugoniot relations are:

$$\rho_0 v_0 = \rho_\infty v_\infty \equiv \dot{m} \tag{1}$$

$$p_0 + \rho_0 v_0^2 = p_\infty + \rho_\infty v_\infty^2 \tag{2}$$

$$h_0 + \frac{v_0^2}{2} = h_\infty + \frac{v_\infty^2}{2} \tag{3}$$

THE HUGONIOT CURVE

THE RANKINE-HUGONIOT RELATION

Equations (1) to (3) may be combined into the Rankine-Hugoniot relation

$$\frac{\gamma-1}{\gamma}\left(\frac{p_\infty}{\rho_\infty}-\frac{p_0}{\rho_0}\right)-\frac{p_\infty-p_0}{2}\left(\frac{1}{\rho_\infty}+\frac{1}{\rho_0}\right)=-(h_\infty-h_1) \tag{4}$$

The difference between a detonation and the shock in an inert gas is in the form of h_∞ .
In a shock the chemical composition remains unchanged, whereas in a detonation the chemical composition changes so that energy is released. Chemical equilibrium is attained after the gas passes through the wave.

- A plot of p_∞ versus $1/\rho_\infty$ for a given value of $(p_0, 1/\rho_0)$ and the heat release $-(h_\infty - h_1)$ is called the Hugoniot curve.
- The Hugoniot curve is the locus of all possible solutions of equations (1) to (3), or equivalently, equation (4).
- The point $(p_0, 1/\rho_0)$ is called the origin of the Hugoniot plot.
- There are two Chapman-Jouget points. They arise from drawing tangents to the Hugoniot curve through the origin of the Hugoniot plot $(p_0, 1/\rho_0)$.

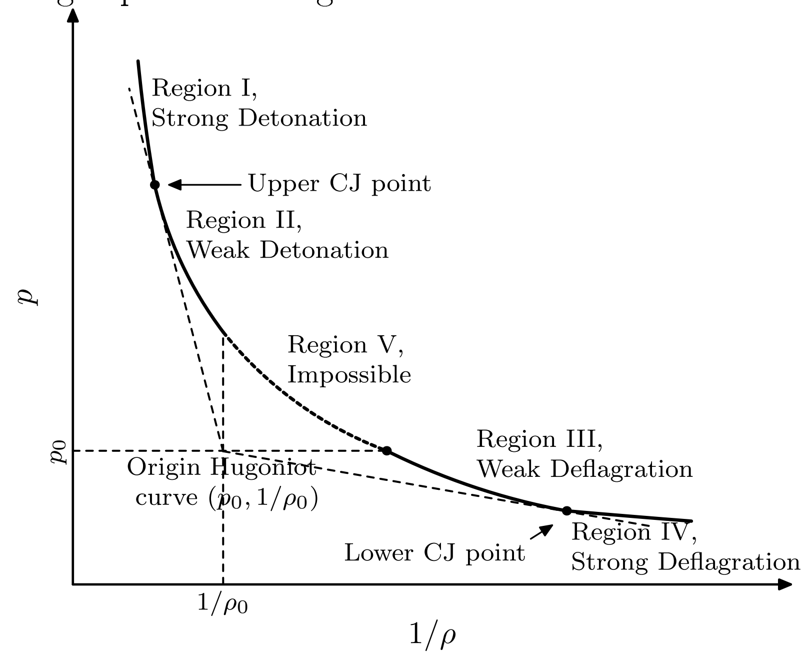

Figure 2: The Rankine-Hugoniot diagram.

THE HUGONIOT CURVE

THE RANKINE-HUGONIOT DIAGRAM

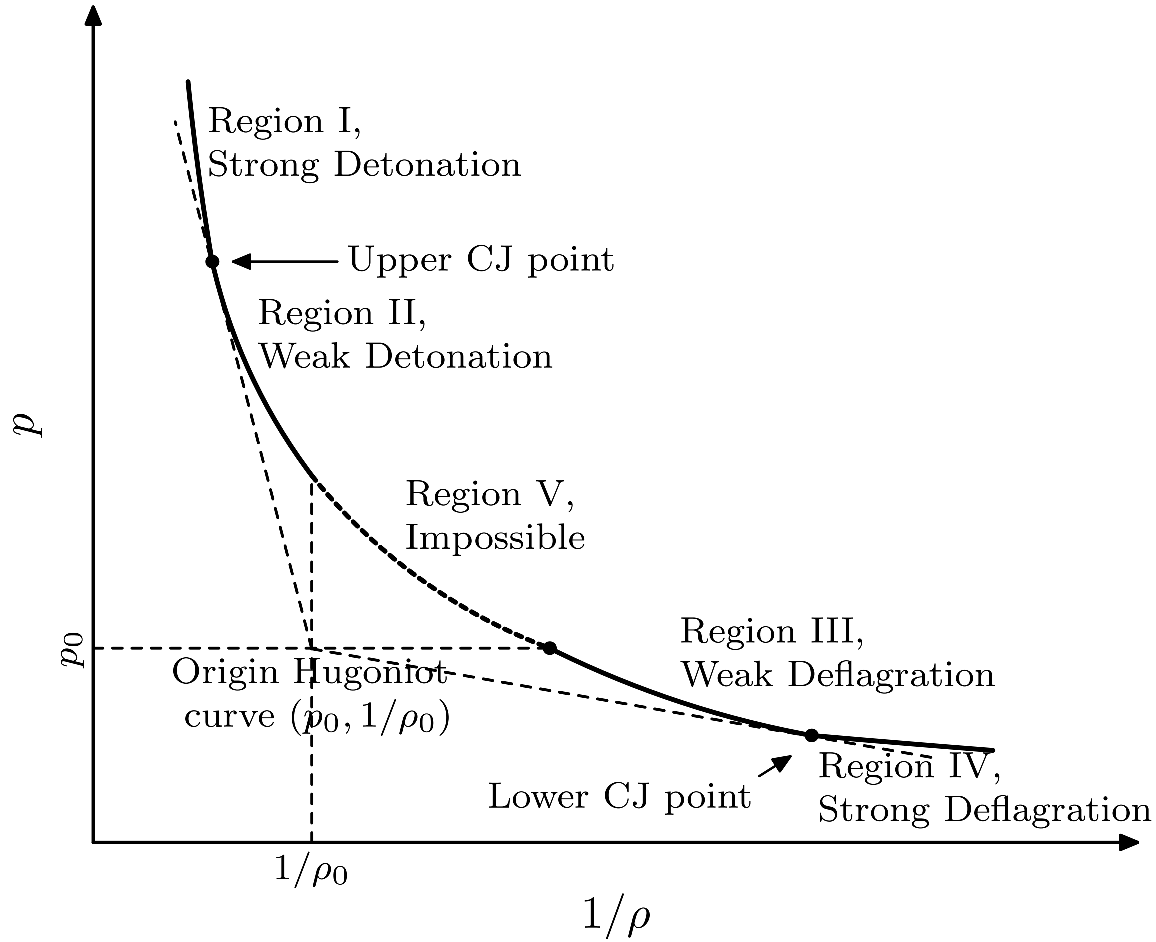

Figure 2: The Rankine-Hugoniot diagram.

THE HUGONIOT CURVE

THE RAYLEIGH-LINE RELATION

Equations (1) and (2) may be combined into the Rayleigh-line relation

$$\rho_0^2 v_0^2 = \frac{p_\infty - p_0}{1/\rho_0 - 1/\rho_\infty} \equiv \dot{m}^2 \tag{5}$$

The Rayleigh-line relation is a criterion to identify regimes within the Hugoniot curve where deflagration and detonation are possible.

- Region I, strong detonation regime.
- Region II, weak detonation regime.
- Region III, weak deflagration regime.
- Region IV, strong deflagration regime.
- In region V, it is seen that $1/\rho_0 - 1/\rho_\infty < 0$ and in $p_0 - p_\infty > 0$. The Rayleigh-line relation implies imaginary values for v_0 (i.e. impossible for deflagration or detonation to exists).

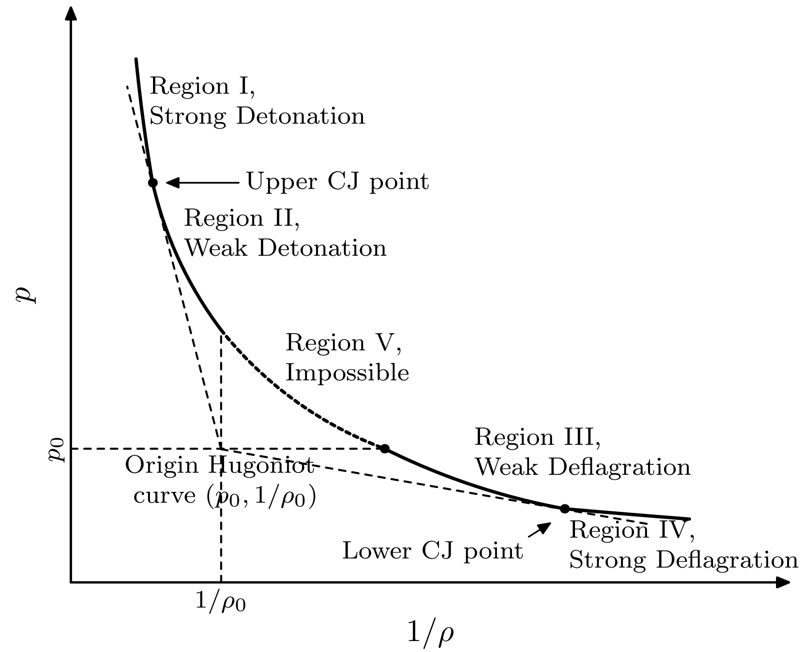

Figure 2: The Rankine-Hugoniot diagram.

THE HUGONIOT CURVE

THE RAYLEIGH-LINE RELATION

Deflagrations are subsonic combustion waves:

- Typical deflagrations propagate at speeds on the order of 1-100 $\mathrm{m\,s^{-1}}$.
- Across a deflagration, the pressure decreases while the volume increases: $p_\infty < p_0$ and $1/\rho_\infty > 1/\rho_0$.
- For deflagrations, the structure of the wave, and turbulent and diffusive processes, determine the propagation speed.

Detonations are supersonic combustion waves:

- Typical detonation waves propagate at a velocity on the order of 2000 $\mathrm{m\,s^{-1}}$.
- Across a detonation, the pressure increases while the volume decreases: $p_\infty > p_0$ and $1/\rho_\infty < 1/\rho_0$.
- For detonations in stoichiometric hydrogen and hydrocarbon fuel-air mixtures: $p_\infty/p_0 = 15 - 20$. For detonations, gas dynamic considerations are sufficient to determine the solution. Chapman (1899) [1] and Jouguet (1905) [2] proposed that detonations travel at one particular velocity, which is the minimum velocity for all the solutions on the detonation branch (the Chapman-Jouget velocity).
- Zeldovich (1940) [3], von Neumann (1943) [4] and Döring (1943) [5] postulated independently that a detonation is a combustion wave being sustained by a shock wave.

THE HUGONIOT CURVE

THE CHAPMAN-JOUGET POINTS

Differentiate the Rankine-Hugoniot relation (4) with respect to ρ_∞ to obtain:

$$\frac{1}{\rho_\infty}\left(\frac{\gamma}{\gamma-1}\right)\frac{dp_\infty}{d(1/\rho_\infty)}+\left(\frac{\gamma}{\gamma-1}\right)p_\infty-\frac{1}{2}(p_\infty-p_0)-\frac{1}{2}\frac{dp_\infty}{d(1/\rho_\infty)}\left(\frac{1}{\rho_\infty}+\frac{1}{\rho_0}\right)=0 \tag{6}$$

and hence:

$$\frac{dp_\infty}{d(1/\rho_\infty)}=\frac{(p_\infty-p_0)-\left(\frac{2\gamma}{\gamma-1}\right)p_\infty}{\left(\frac{2\gamma}{\gamma-1}\right)\frac{1}{\rho_\infty}-\left(\frac{1}{\rho_\infty}+\frac{1}{\rho_0}\right)} \tag{7}$$

The slopes at the Chapman-Jouget points are:

$$\left.\frac{dp_\infty}{d(1/\rho_\infty)}\right|_{\mathrm{CJ}}=\frac{p_\infty-p_0}{(1/\rho_\infty)-(1/\rho_0)} \tag{8}$$

From (7) and (8):

$$\frac{p_\infty-p_0}{(1/\rho_\infty)-(1/\rho_0)}=-\gamma\rho_\infty p_\infty-p_0 \tag{9}$$

The Rayleigh-line is tangent to the Hugoniot curve at the Chapman-Jouget points. From (9) and the Rayleigh-line relation (5):

$$v_\infty^2=\frac{\gamma p_\infty}{(\rho_\infty)}=c_\infty^2 \quad \text{or} \quad |v_\infty|=c_\infty \tag{10}$$

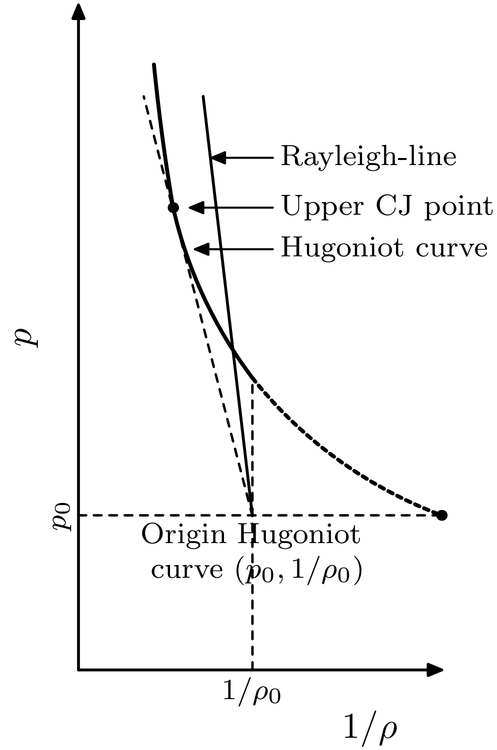

Figure 3: The upper Chapman-Jouget point and the tangency condition between the Rayleigh-line and the Hugoniot curve.

Equation (10) implies that the Mach number behind the shock wave is unity ($\mathrm{Ma}_\infty = 1$) at the Chapman-Jouget points.

THE HUGONIOT CURVE

THE CHAPMAN-JOUGET POINTS

Table 1: Experimentally observed conditions of pressure (p_∞), temperature (T_∞), and velocity (v_∞) at the upper Chapman-Jouget point. Initial conditions $p_0 = 1\,\text{bar}$ and $T_0 = 291\,\text{K}$. After: Hirschfelder, Curtiss & Bird (1967) [6].

Explosive mixture	pressure p_∞ (bar)	temperature T_∞ (K)	velocity v_∞ ($\text{m}\,\text{s}^{-1}$)
$(2\,H_2 + O_2)$	18.1	3583	2819
$(2\,H_2 + O_2) + 5\,O_2$	14.1	2620	1700
$(2\,H_2 + O_2) + 5\,N_2$	14.4	2685	1822
$(2\,H_2 + O_2) + 4\,H_2$	16.0	2976	3527
$(2\,H_2 + O_2) + 5\,He_2$	16.3	3097	3160
$(2\,H_2 + O_2) + 5\,Ar_2$	16.3	3097	1700

THE CHAPMAN-JOUGET DETONATION WAVE VELOCITY

DERIVATION OF AN ITERATIVE PROCEDURE

A procedure for estimating the Chapman-Jouget velocity from the thermodynamic properties of the unreacted mixture may be derived as follows. The sonic velocity behind a detonation wave is:

$$c_\infty = \sqrt{\left[\frac{\partial p_\infty}{\partial \rho_\infty}\right]_s} \tag{11}$$

Because $u_\infty = c_\infty$ at the upper Chapman-Jouget point, the condition of mass conservation (1) across the shock wave and equation (11) lead to:

$$u_0 = \frac{1}{\rho_0} c_\infty \rho_\infty = \frac{1}{\rho_0}\sqrt{\rho_\infty^2 \left[\frac{\partial p_\infty}{\partial \rho_\infty}\right]_s} = \frac{1}{\rho_0}\sqrt{-\left[\frac{\partial p_\infty}{\partial (1/\rho_\infty)}\right]_s} \tag{12}$$

Differentiation of the isentropic relation for the burned gas,

$$p_\infty \left(\frac{1}{\rho_\infty}\right)^{\gamma_\infty} = \text{constant} \quad \Longrightarrow \quad -\left[\frac{\partial p_\infty}{\partial (1/\rho_\infty)}\right]_s = \frac{\gamma_\infty p_\infty}{1/\rho_\infty} \tag{13}$$

and substitution into equation (12) gives

$$\boxed{u_0 = p_\infty \frac{1/\rho_0}{1/\rho_\infty}\sqrt{\gamma_\infty p_\infty \frac{1}{\rho_\infty}} = \frac{\rho_\infty}{\rho_0}\sqrt{\gamma_\infty R_\infty T_\infty}} \quad \text{or} \quad \boxed{\rho_0^2 u_0^2 = \gamma_\infty p_\infty \rho_\infty} \tag{14}$$

after application of the ideal gas law.

THE CHAPMAN-JOUGET DETONATION WAVE VELOCITY

DERIVATION OF AN ITERATIVE PROCEDURE

Derive an equivalent Rankine-Hugoniot relation by combining Kirckhoff's law with the ideal gas law,

$$\frac{p}{\rho} = \frac{\gamma - 1}{\gamma} \sum_{i=1}^{N} Y_i \left[h^{\circ}_{f\,i} + \int_{T^{\circ}}^{T} \hat{C}_{P\,i}(T)\, dT \right] \quad \Longrightarrow \quad h = h^{\circ} + \left(\frac{\gamma}{\gamma - 1} \right) \frac{p}{\rho} \tag{15}$$

and substituting this into the conventional Rankine-Hugoniot relation (4):

$$h_{\infty} - h_0 = \frac{1}{2}(p_{\infty} - p_0) \left(\frac{1}{\rho_{\infty}} + \frac{1}{\rho_0} \right) \tag{16}$$

Because $h = e + (p/\rho)$,

$$h_{\infty} - h_0 = (e_{\infty} - e_0)(p_{\infty} - p_0) \left(\frac{p_{\infty}}{\rho_{\infty}} + \frac{p_0}{\rho_0} \right) \tag{17}$$

so that (16) becomes

$$e_{\infty} - e_0 = \frac{1}{2}(p_{\infty} - p_0) \left(\frac{1}{\rho_{\infty}} + \frac{1}{\rho_0} \right) - \left(\frac{p_{\infty}}{\rho_{\infty}} + \frac{p_0}{\rho_0} \right) \tag{18}$$

$$\boxed{e_{\infty} - e_0 = \frac{1}{2}(p_{\infty} - p_0) \left(\frac{1}{\rho_0} - \frac{1}{\rho_{\infty}} \right)} \tag{19}$$

THE CHAPMAN-JOUGET DETONATION WAVE VELOCITY

DERIVATION OF AN ITERATIVE PROCEDURE

Substitute equation (14) into the Rayleigh-line relation (5):

$$\frac{1}{\rho_\infty} + \frac{1}{\rho_0} = -\frac{p_\infty - p_0}{\gamma_\infty p_\infty \rho_\infty} \tag{20}$$

and combine this result with equation (19) to obtain

$$\boxed{e_\infty - e_0 = \frac{p_\infty^2 - p_0^2}{\gamma_\infty p_\infty \rho_\infty}} \tag{21}$$

Multiply equation (20) by $(p_\infty + p_0)$ to have

$$\boxed{(p_\infty - p_0)\left(\frac{1}{\rho_\infty} + \frac{1}{\rho_0}\right) = \frac{(p_\infty^2 - p_0^2)}{\gamma_\infty p_\infty \rho_\infty}} \tag{22}$$

Equations (19), (21) and (22) form the design basis of an iterative procedure to determine the Chapman-Jouget velocity from the thermodynamic properties of the unreacted mixture.

For a detonation wave $p_\infty \gg p_0$ so that equations (21) and (22) may be rewritten into an approximate Rankine-Hugoniot relation (23) and an approximate Rayleigh-line relation (24):

$$\boxed{e_\infty - e_0 \approx \frac{p_\infty^2 - p_0^2}{\gamma_\infty p_\infty \rho_\infty} = \frac{R_\infty T_\infty}{2\gamma_\infty}} \tag{23}$$

$$\boxed{\left(\frac{\rho_\infty}{\rho_0}\right)^2 \left(1 + \frac{1}{\gamma_\infty} - \frac{R_0 T_0}{R_\infty T_\infty}\right)\left(\frac{\rho_\infty}{\rho_0}\right) - \frac{R_0 T_0}{R_\infty T_\infty} = 0} \tag{24}$$

THE CHAPMAN-JOUGET DETONATION WAVE VELOCITY

DERIVATION OF AN ITERATIVE PROCEDURE

The iterative procedure to determine the Chapman-Jouget velocity from the thermodynamic properties of the unreacted mixture is as follows.

1. Assume p_∞.
2. Assume T_∞.
3. Calculate the equilibrium composition based on p_∞ and T_∞.
4. From the equilibrium composition, determine γ_∞, R_∞ and e_∞.
5. Verify whether γ_∞, R_∞ and e_∞ at the assumed temperature T_∞ satisfies the approximate Rankine-Hugoniot relation (23).
   - If equation (23) is satisfied, proceed to step 6.
   - If not, then reassume a new p_∞ and return to step 2.
6. Solve the approximate Rayleigh-line relation (24) for ρ_∞/ρ_0.
7. Find p_∞ from the equation of state, e.g. the ideal gas law

$$p_\infty = \left(\frac{\rho_\infty}{\rho_0}\right)\left(\frac{R_\infty T_\infty}{R_0 T_0}\right) p_0 \qquad (25)$$

   - If the calculated p_∞ equals the assumed p_∞, the iteration sequence has completed. Proceed to step 8.
   - If not, then return to step 1 and assume a new p_∞.
8. Calculate the Chapman-Jouget velocity, v_∞, from equation (14).

DETONATION WAVE STRUCTURE

THE ZELDOVICH-VON NEUMANN-DÖRING THEORY OF DETONATION (ONE-DIMENSIONAL WAVE STRUCTURE)

The simplest model of the structure of a detonation wave (the ZND structure) consists of a shock wave coupled to a reaction zone. Zeldovich (1940), von Neumann (1943) and Döring (1943) were the first who postulated this view.

- The shock wave compresses and heats up the gas, which reacts after an induction period.
- The reaction triggers a volumetric expansion of the gas, which drives the shock wave.

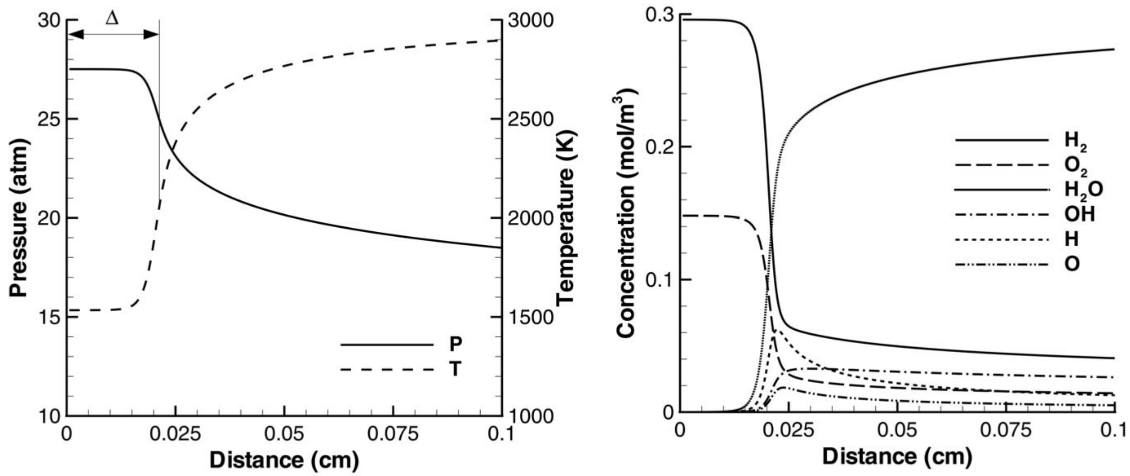

Figure 4: ZND profile of a detonation wave in stoichiometric hydrogen-air mixture ignited at 1 bar and 300 K. Δ denotes the induction zone length.

DETONATION WAVE STRUCTURE

MULTI-DIMENSIONAL WAVE STRUCTURE

Detonation waves have a multidimensional structure.

- They consist of a leading shock waves, triple points, and transverse waves.
- The wave structure has a cellular pattern.
- The structure of a detonation wave is correlated with detonation limits.
- The cellular structure left behind on sooted foils is a record of the triple point trajectory.
- Empirical correlations exist between cell width and detonation limits.

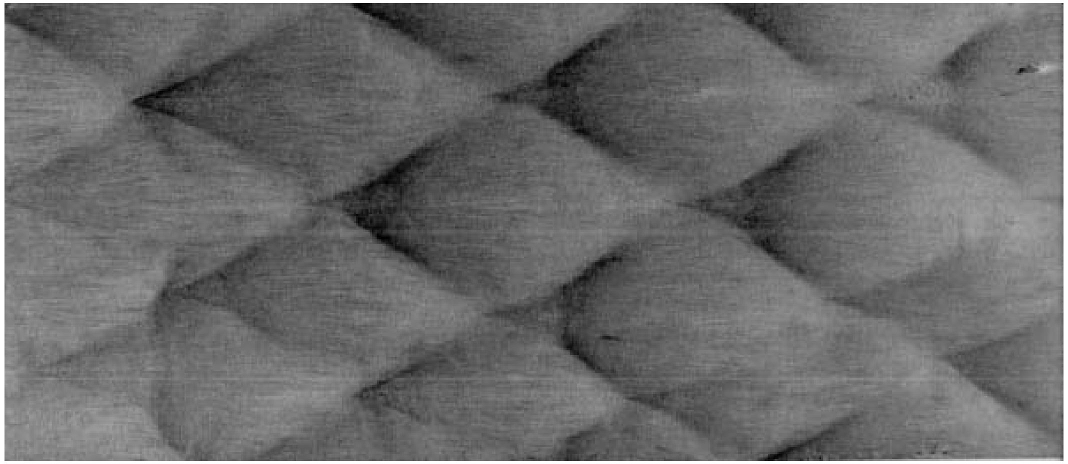

Figure 5: Cellular structure imprinted on a sooted foil record by the detonation of a $2H_2 + O_2 + 17Ar$ mixture, ignited at 20 kPa and 295 K. After Austin (2003) [7].

DETONATION WAVE STRUCTURE

MULTI-DIMENSIONAL WAVE STRUCTURE

a) 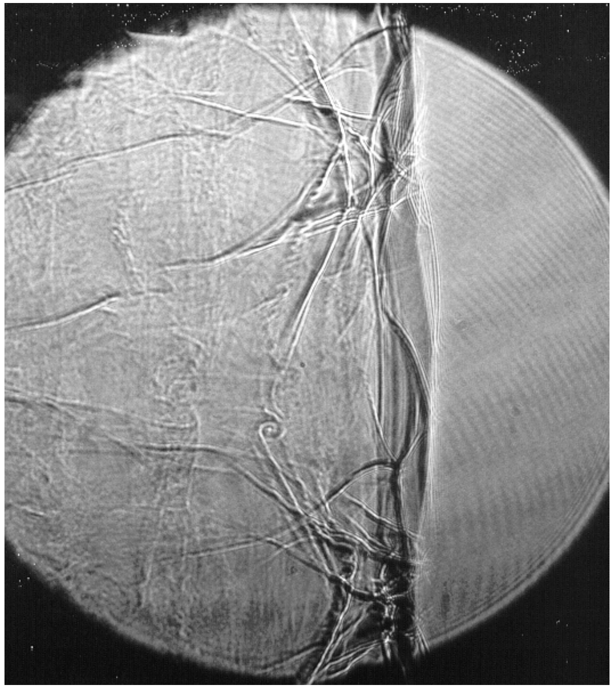

b) 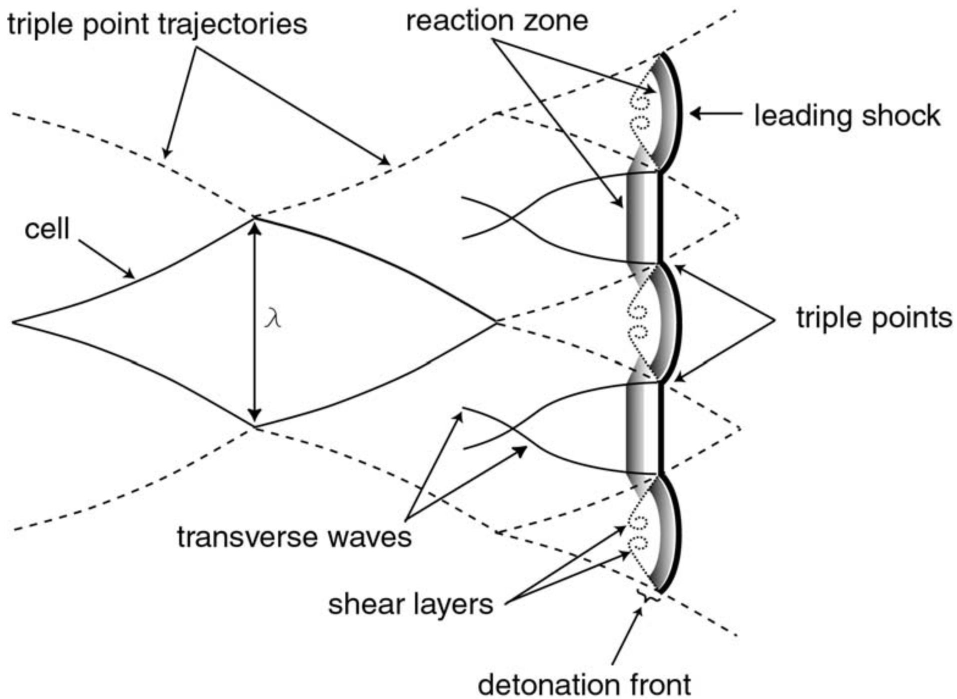

Figure 6: a) Structure of a detonation wave in a $2H_2 + O_2 + 20Ar$ mixture at 20 kPa and 295 K (after Akbar (1997) [8]). b) Formation of the cellular structure on a sooted foil record by a detonation wave (after Winterberger & Shepherd (2004)).

DETONATION WAVE STRUCTURE

MULTI-DIMENSIONAL WAVE STRUCTURE

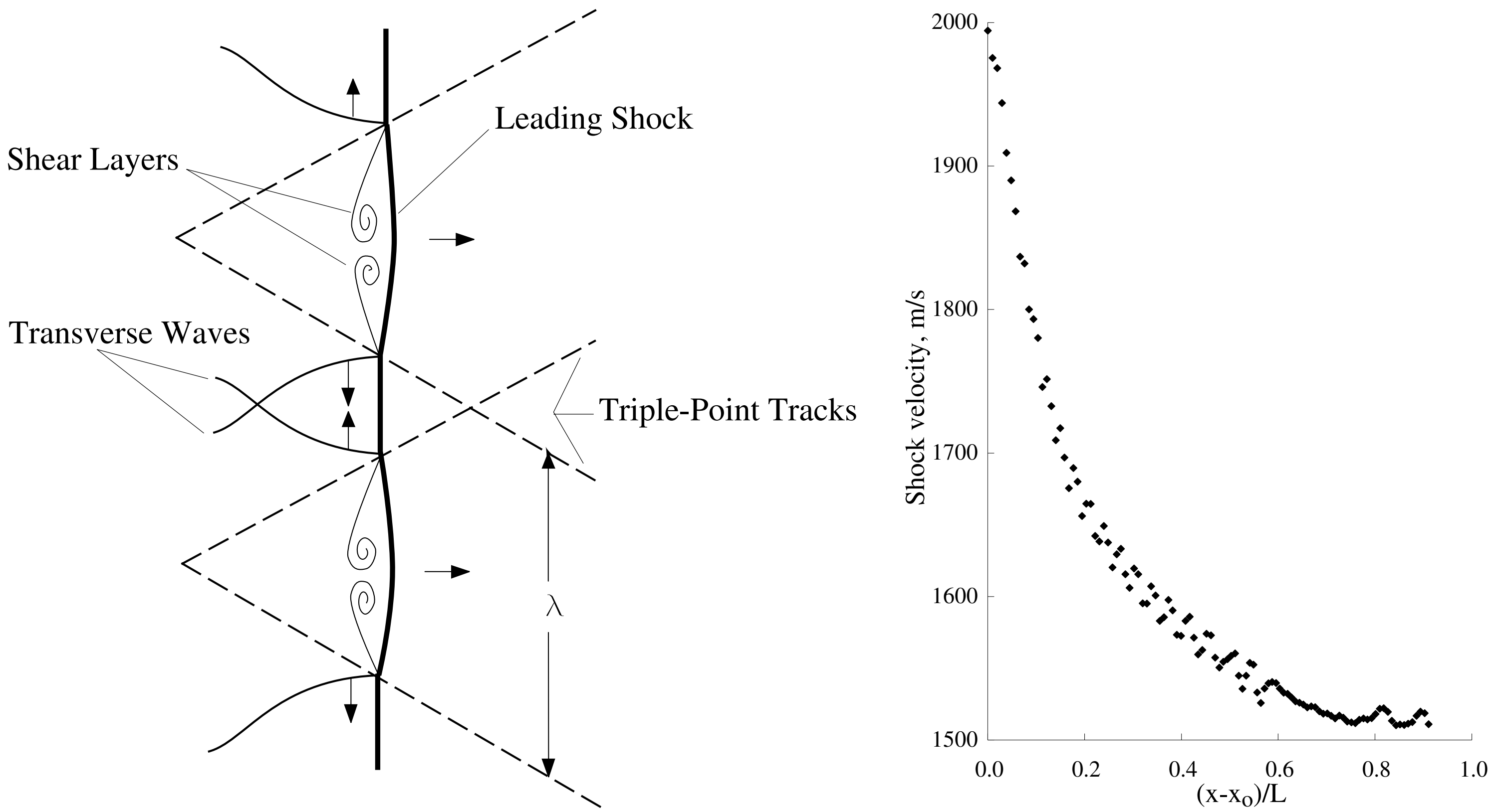

Figure 7: Morphology of a multi-dimensional detonation front propagating from left to right. After: Austin (2003) [7], Eckett(2000) [9], and Pintgen, Eckett, Austin & Shepherd (2003) [10].

DETONATION WAVE STRUCTURE

MULTI-DIMENSIONAL WAVE STRUCTURE

Morphology of a multi-dimensional detonation front:

- Triple points exist at the junction of the leading shock front and a transverse wave.
- The pattern observed on soot foils is a history of the triple point tracks in the propagating detonation front. Urtiew and Oppenheim (1966) [11] have shown that the tracks are closely related with the triple points on the detonation front.
- The precise physical mechanism by which the tracks are made in the soot layer is still unclear!
- The width of cells that appear on the foil are a measure of the spacing of the transverse waves in the detonation front. This global length scale, referred to as the detonation cell width, λ, can not in general be calculated a priori but may be related to the induction zone length, Δ, by a constant of proportionality ,A. More specifically,

$$\lambda = A\,\Delta \tag{26}$$

- The constant A depends on the fuel-oxidiser-inert type (Westbrook (1982) [12]) and also varies with the equivalence ratio (Shepherd (1986) [13, 14]).
- The induction zone length can be empirically related to dynamic parameters such as the critical initiation energy (Lee (1984) [15]).

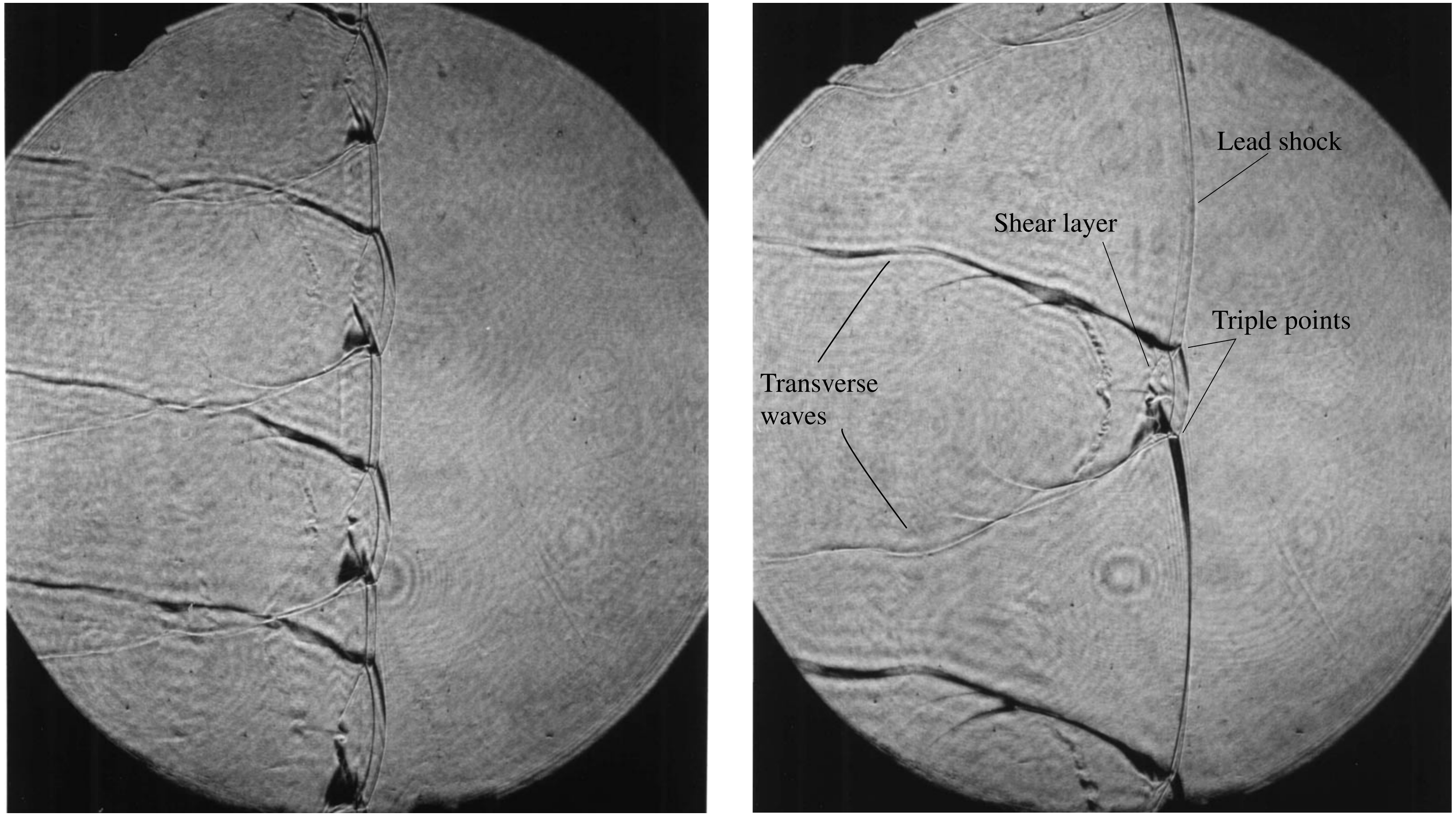

Figure 8: Schlieren images of (left) a $2H_2$-O_2-12Ar detonation, p_0=20 kPa, and (right) a $2H_2$-O_2-17Ar detonation, p_0=20 kPa (after Austin (2003) [7]).

DETONATION WAVE STRUCTURE

MULTI-DIMENSIONAL WAVE STRUCTURE

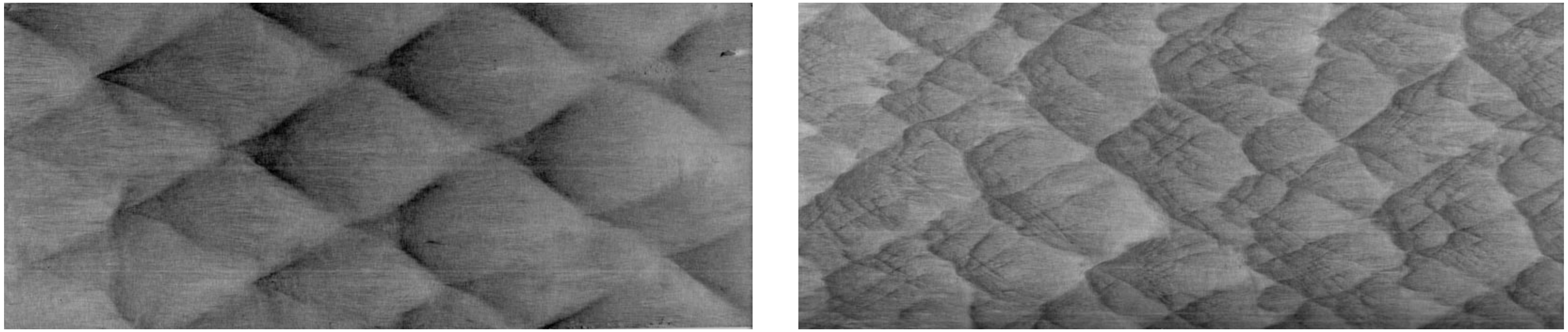

Figure 9: Sample soot foils with (left) regular cellular structure in $2H_2$-O_2-17Ar, and (right) irregular structure in C_3H_8-$5O_2$-$9N_2$. p_0=20 kPa and image height is 152 mm (after Austin (2003) [7]).

DETONATION WAVE STRUCTURE

MULTI-DIMENSIONAL WAVE STRUCTURE

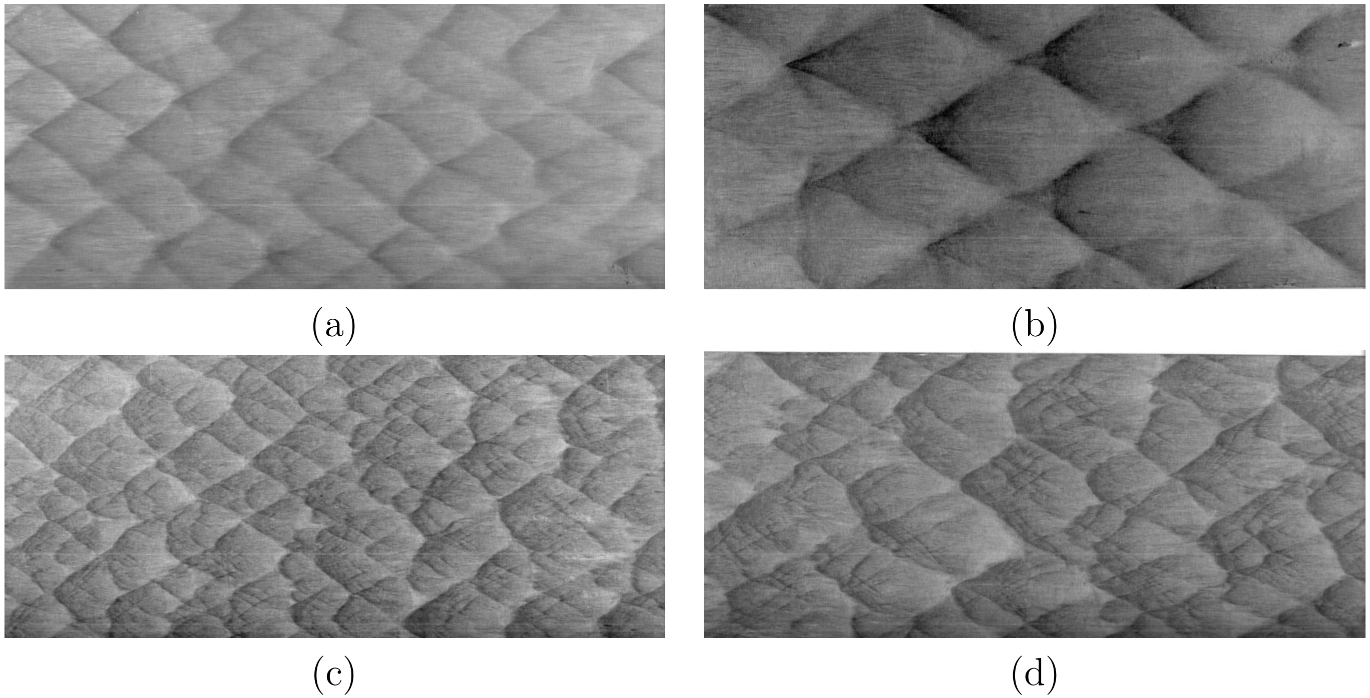

Figure 10: Sample soot foils from weakly unstable (a) $2H_2$-O_2-$12Ar$ detonations, (b) $2H_2$-O_2-$17Ar$ detonations, (c) H_2-N_2O-$1.33N_2$ detonations, and (d) C_3H_8-$5O_2$-$9N_2$ detonations. (after Austin (2003) [7]).

DETONATION WAVE STRUCTURE

MULTI-DIMENSIONAL WAVE STRUCTURE

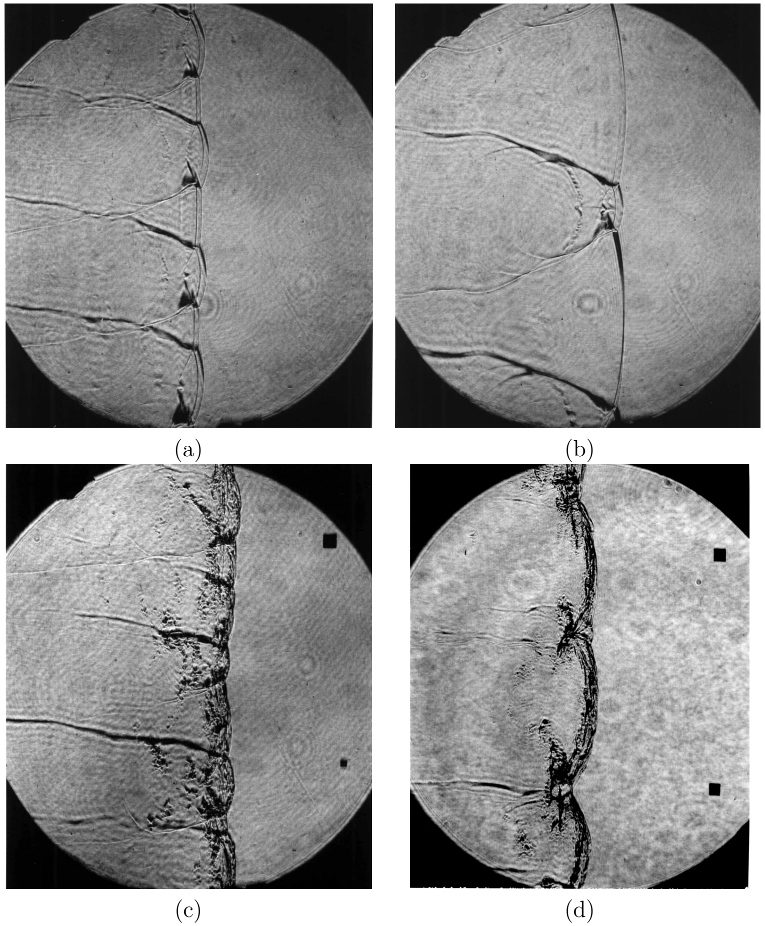

Figure 11: Schlieren images of weakly unstable (a) $2H_2$-O_2-12Ar detonations, (b) $2H_2$-O_2-17Ar detonations, (c) H_2-N_2O-1.77N_2 detonations, and (d) C_2H_4-3O_2-9N_2 detonations. p_0=20 kPa. (after Austin (2003) [7]).

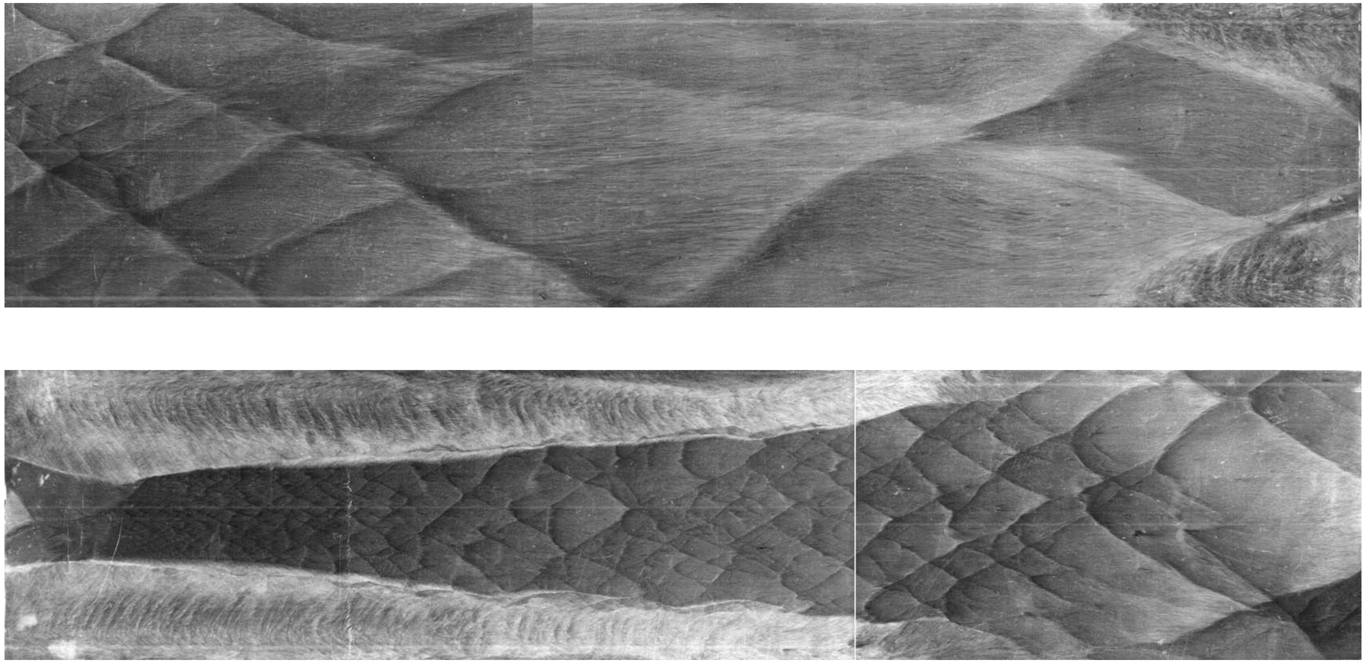

Figure 12: Sample soot foils from highly unstable CH_4-$2O_2$-0.2 Air detonations (after Austin (2003) [7]).

DETONATION CELL SIZE

DEPENDENCE ON COMPOSITION AND TEMPERATURE

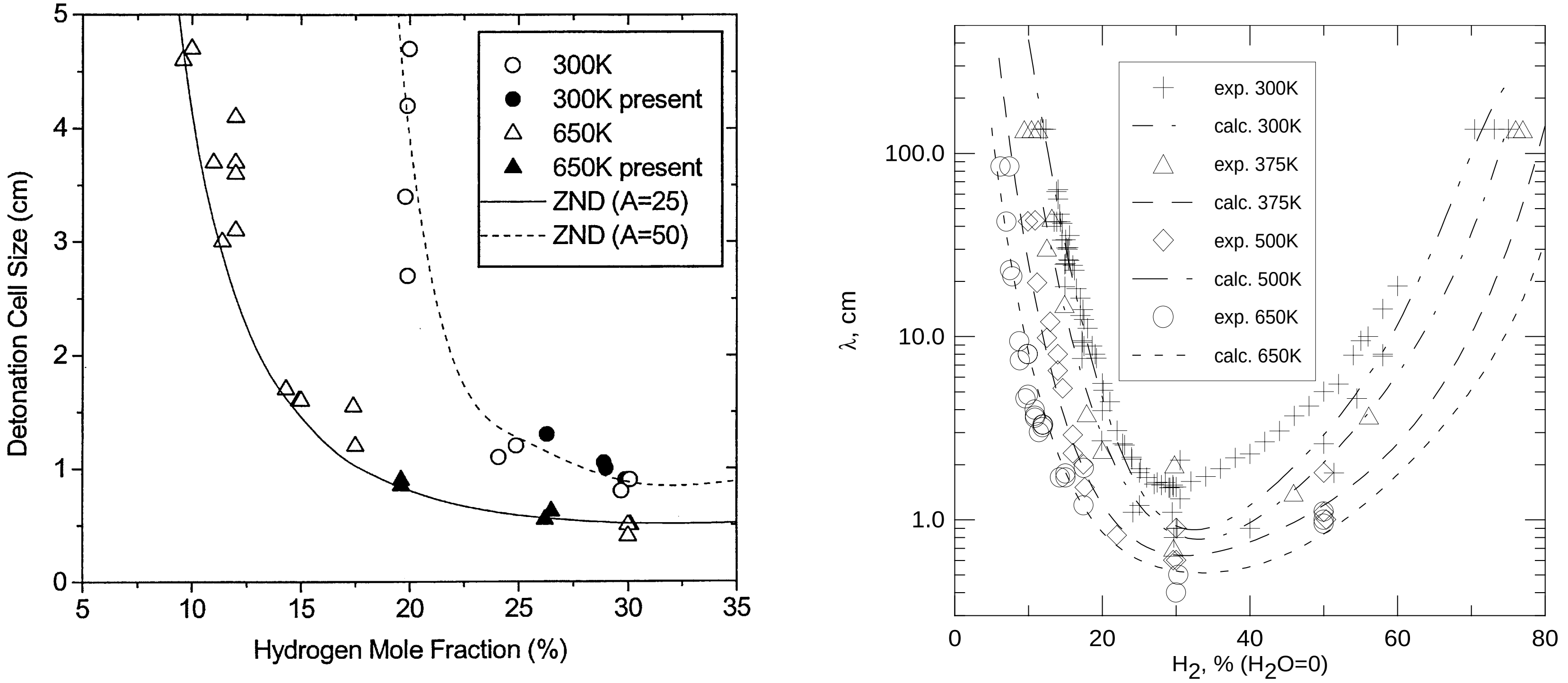

Figure 13: Detonation cell-size for hydrogen-air mixtures at different initial temperatures (after Breitung *et al.*(2000) [16]) and Ciccarelli (2002) [17].

DETONATION CELL SIZE

COMPARISON BETWEEN HYDROGEN AND HYDROCARBON FUELS

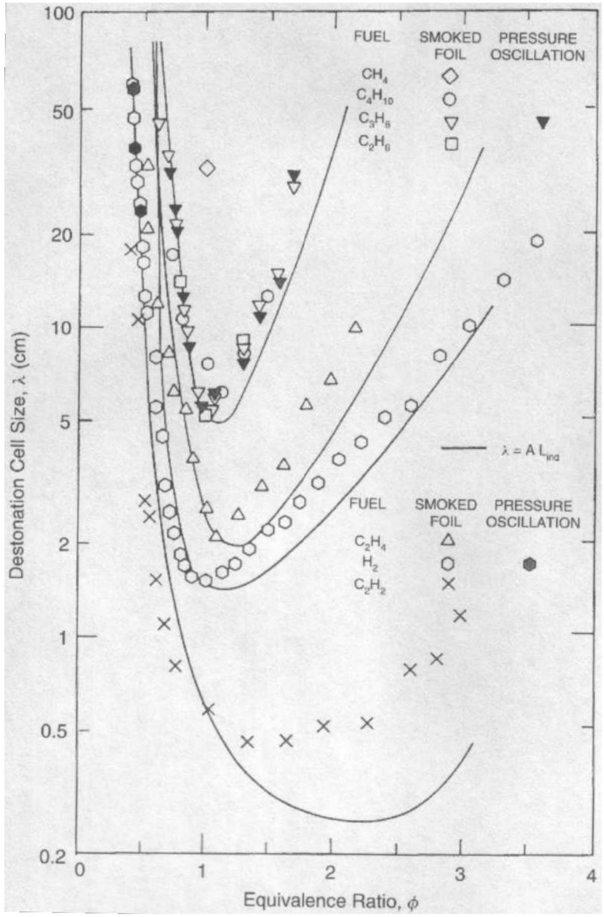

Figure 14: Detonation cell-size of different fuels (after Knystautas *et al.* [18]).

RELATIONSHIP BETWEEN DETONATION ENERGY AND DETONATION CELL SIZE

COMPARISON BETWEEN HYDROGEN, OTHER FUELS, AND EXPLOSIVES

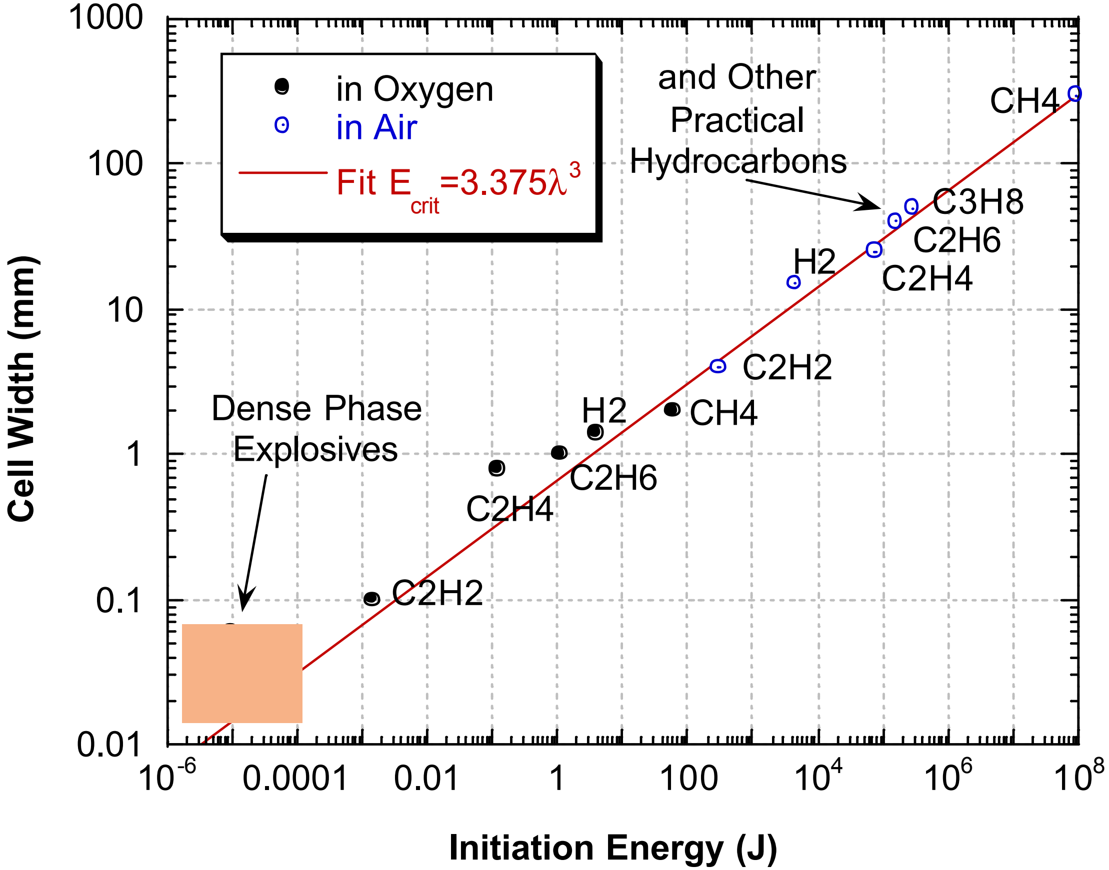

Figure 15: Detonation cell-size of different fuels (after Schauer *et al.* [19]).

References

[1] Chapman D.L. On the rate of explosion in gases. *Physics of Fluids*, 47:90–104, 1899.

[2] Jouguet E. On the propagation of chemical reactions in gases. *Journal de Mathematiques Pures et Appliquees*, 1:347–425, 1906.

[3] Zeldovich Ya.B. On the theory of the propagation of detonation in gaseous systems. *Journal of Experimental and Theoretical Physics*, 10:542–568, 1940.

[4] Neumann J. von. Theory of detonation waves. In A.H. Taub, editor, *John von Neumann, collected works*, volume 6 of *Theory of games, astrophysics, hydrodynamics and meteorology*. Pergamon, Oxford, 1942.

[5] Döring W. Uber den detonationvorgangin gases. *Ann. Phys. Lpz.*, 43:421–436, 1943.

[6] Hirschfelder J.O., Curtiss C.F., and Bird R.B. *The molecular theory of gases and liquids*. John Wiley & Sons, New York, fourth edition, 1967.

[7] Austin J.M. *The Role of Instability in Gaseous Detonation*. PhD thesis, California Institute of Technology, California, United States of America, May 2003.

[8] Akbar R. *Mach reflection of gaseous detonations*. PhD thesis, Rensselaer Polytechnic Institute, New York, United States of America, August 1997.

[9] Eckett C. A., Quirk J. J., and Shepherd J. E. The role of unsteadiness in direct initiation of gaseous detonations. *Journal of Fluid Mechanics*, 421:147–183, 2000.

[10] Pintgen F., Eckett C.A., Austin J.M., and Shepherd J.E. Direct observations of reaction zone structure in propagating detonations. *Combustion and Flame*, 133:211–229, 2003.

[11] Urtiew P.A. and Oppenheim A.K. Experimental observations of transition to detonation in explosive gas. *Proceedings of the Royal Society of London, Series A: Mathematical and Physical Sciences*, 295:13–38, 1966.

[12] Westbrook C.K. Chemical-kinetics of hydrocarbon oxidation in gaseous detonation. *Combustion and Flame*, 46:191–216, 1982.

[13] Shepherd J. Chemical kinetics of hydrogen-air-diluent detonations. *Progress in Aeronautics and Astronautics*, 106:263–293, 1986.

[14] Shepherd J., Moen I.O., Murray S., and Thibault P. Analysis of the cellular structure of detonations. In *Proceedings of the Twenty-First Symposium (International) on Combustion*, pages 1649–1658, Pittsburgh, 1986. The Combustion Institute.

[15] Lee J.H.S. Dynamic parameters of gaseous detonations. *Annual Review of Fluid Mechanics*, 16:311–336, 1984.

[16] Breitung W., Chan C.K., Dorofeev S.B., Eder A., Gelfand B.E., Heitsch M., Klein R., Malliakos A., Shepherd J.E., Studer E., and Thibault P. Flame acceleration and deflagration to detonation transition in nuclear safety. State-of-the-art report by a group of experts, OECD Nuclear Energy Agency, August 2000.

[17] Ciccarelli G. Critical tube measurements at elevated initial mixture temperatures. *Combustion Science and Technology*, 174:173–183, 2002.

[18] Knystautas R., Lee J.H.S., Moen I.O., and Wagner H.Gh. Direct initiation of spherical detonation by a hot turbulent gas jet. In *Proceedings of the Seventeenth Symposium (International) on Combustion*, pages 1235–1245, Pittsburgh, 1979. The Combustion Institute.

[19] Schauer F.R., Miser C.L., Tucker K.C., Bradley R.P., and Hoke J.L. Detonation initiation of hydrocarbon-air mixtures in a pulsed detonation engine. AIAA-paper 2005-1343, 2005.